Published in final edited form as:

Science. 2017 June 23; 356(6344): 1276–1280. doi:10.1126/science.aam6203.

Metalloprotein entatic control of ligand-metal bonds quantified by ultrafast x-ray spectroscopy

Michael W. Mara[1,2,*], **Ryan G. Hadt**[1,†], **Marco Eli Reinhard**[3], **Thomas Kroll**[2,4], **Hyeongtaek Lim**[1,2], **Robert W. Hartsock**[3], **Roberto Alonso-Mori**[4], **Matthieu Chollet**[4], **James M. Glownia**[4], **Silke Nelson**[4], **Dimosthenis Sokaras**[2,4], **Kristjan Kunnus**[3], **Keith O. Hodgson**[1,2], **Britt Hedman**[2], **Uwe Bergmann**[3,4], **Kelly J. Gaffney**[2,3], and **Edward I. Solomon**[1,2,‡]

[1]Department of Chemistry, Stanford University, Stanford, CA 94305, USA

[2]Stanford Synchrotron Radiation Lightsource, SLAC National Accelerator Laboratory, Stanford University, 2575 Sand Hill Road, Menlo Park, CA 94025, USA

[3]PULSE Institute, SLAC National Accelerator Laboratory, Stanford University, Stanford, CA 94305, USA

[4]Linac Coherent Light Source, SLAC National Accelerator Laboratory, Stanford University, Menlo Park, CA 94025, USA

Abstract

The multifunctional protein cytochrome c (cyt c) plays key roles in electron transport and apoptosis, switching function by modulating bonding between a heme iron and the sulfur in a methionine residue. This Fe–S(Met) bond is too weak to persist in the absence of protein constraints. We ruptured the bond in ferrous cyt c using an optical laser pulse and monitored the bond reformation within the protein active site using ultrafast x-ray pulses from an x-ray free-electron laser, determining that the Fe–S(Met) bond enthalpy is ~4 kcal/mol stronger than in the absence of protein constraints. The 4 kcal/mol is comparable with calculations of stabilization effects in other systems, demonstrating how biological systems use an entatic state for modest yet accessible energetics to modulate chemical function.

Cytochrome c (cyt c) is a metalloprotein that plays dual roles in biology as an electron transfer (ET) agent and a peroxidase, serving as a model protein for probing structure/function relationships in biological inorganic chemistry. The cyt c active site contains a six-coordinate, low-spin (LS) heme iron with axial His18 and Met80 ligands, the latter of which is particularly vital to protein function (1–3). The prevalence of metal-thioether bonds in ET proteins has inspired interest in understanding their contributions to function. Across copper

‡Corresponding author. edward.solomon@stanford.edu.
*Present address: Department of Chemistry, University of California, Berkeley, Berkeley, CA 94720, USA.
†Present Address: Chemical Sciences and Engineering Division, Argonne National Laboratory, Lemont, IL 60439, USA.

SUPPLEMENTARY MATERIALS
www.sciencemag.org/content/356/6344/1276/suppl/DC1
Materials and Methods
Supplementary Text
Figs. S1 to S15
References (*41–46*)

and iron ET proteins, the S(Met) bond contributes a relative energetic stabilization of the oxidized over the reduced state. Temperature-dependent studies of the Cu–S(Met) bond in nitrite reductase (NiR), a type one (T1) copper protein, indicated that the bond strength in the cupric state is low (~5 kcal/mol), and thus this bond should not be present at physiological temperatures (4). This finding suggested a possible role of the protein environment in keeping the thioether-metal bond intact by opposing the entropic contribution to the free energy of ligand loss. This protein control of the active site is referred to as the entatic/rack-induced state (4, 5) and is thought to be integral in regulating the chemical properties of metalloproteins. This concept, however, has not been demonstrated experimentally or quantified.

While functioning as an ET protein, the Fe–S(Met) bond keeps the metal low-spin while the heme iron site shuttles between Fe(II) and Fe(III), which maintains a low inner-sphere reorganization energy for rapid ET (3, 4, 6). However, cyt c can also function as a peroxidase, which requires loss of the Fe(III)–S(Met) bond to open a ligand binding site for catalysis (7, 8). This peroxidase function plays an important signaling role in apoptosis, during which the peroxidation of cardiolipin (CL), a lipid in the inner mitochondrial membrane, is followed by expulsion of cyt c into the cytosol (7, 8). Thus, the regulation of the Fe–S(Met) bond in cyt c is extremely important for cellular functions promoting life (oxidative phosphorylation in respiration) and death (peroxidation in apoptosis).

Initially, the Fe(II)–S(Met) bond in cyt c was thought to be stronger than the Fe(III)–S(Met) bond because of the shorter Fe–S(Met) bond in the reduced state [determined by means of extended x-ray absorption fine structure (EXAFS)] (9), ligand competition (10), the temperature dependence of the Fe–S(Met) bond loss (11, 12), and the decrease in E^0 when the Fe–S(Met) bond is lost (13). However, in solution the Met ligand is replaced by a different protein residue or H_2O, complicating bond strength measurements. Moreover, a direct spectroscopic study of the Fe–S(Met) bond by 1s2p resonant inelastic x-ray scattering (RIXS) coupled to density functional theory (DFT) calculations revealed that in the absence of protein constraints, the Fe(II)–S(Met) bond (2.6 kcal/mol) is weaker than the Fe(III)–S(Met) bond (5.9 kcal/mol); furthermore, the Fe(II)–S(Met) bond enthalpy (ΔH) is less than $T\Delta S$ at room temperature (RT), where T is the temperature and ΔS is the entropy (14). In a similar fashion to T1 Cu (and the binuclear Cu_A) ET enzymes (15, 16), the metal–S(Met) bond in cyt c is retained under physiological conditions. This constraint necessitates the presence of a protein entatic state in cyt c that is vital to ET function but weak enough to be lost for catalysis in apoptosis.

Visible light excitation of either the heme Soret (B-band) or Q-bands (α/β-bands) of ferrous cyt c results in ultrafast photodissociation of an axial ligand; this ligand loss and subsequent geminate recombination has been analyzed by using various ultrafast spectroscopic techniques, elucidating the reaction coordinate on the femtosecond and picosecond time scales (17–19). The results from optical transient absorption (OTA), time-resolved resonance Raman (TR^3), and fluorescence upconversion measurements of ferrous cyt c are consistent, indicating the formation of a five-coordinate, high-spin (HS) Fe(II) site on the subpicosecond time scale and subsequent geminate recombination with a lifetime of 5 to 7 ps. Previous studies have also focused on localized heating and heat dissipation from the

active site in cyt c after photo-excitation (20–22). TR^3 measurements showed that loss of the axial ligand places the heme in a vibrationally hot transient state, and intramolecular vibrational energy redistribution (IVR) is complete within ~1 to 2 ps, resulting in a hot five-coordinate ground state (19). Vibrational cooling can be approximated as an exponential process with a lifetime of 6.8 ps, which is consistent with molecular dynamics simulations that show that the increased heme kinetic energy upon photo-excitation dissipates into the bulk protein, with a calculated lifetime of 6.4 ps (22). Last, the TR^3 measurements revealed a 216-cm^{-1} band in photoexcited ferrous cyt c, assigned as an Fe-His stretch on the basis of the energy of this vibration observed for deoxyhemoglobin (23), suggesting that the Fe–S(Met) bond is broken upon photoexcitation (19).

Ultrafast x-ray spectroscopy is a powerful tool for applying the principles underlying ultrafast optical methods in order to directly probe the properties of a transition metal site (24, 25). The Linac Coherent Light Source (LCLS) x-ray free-electron laser (XFEL) provides extremely intense, ultrafast x-ray pulses to probe photo-induced dynamics on the femtosecond to picosecond time scales. In this study, we used ultrafast Fe K-edge x-ray absorption near-edge spectroscopy (XANES) (24) to directly probe the ligand environment of the iron, and we used Fe Kβ x-ray emission spectroscopy (XES) (25) to directly probe its spin state. Thus, these methods in tandem unambiguously revealed the geometric and electronic structure dynamics of photoexcited ferrous cyt c, providing a direct correlation between axial ligand rebinding to the Fe and the temperature decay. The latter enabled experimental quantification of a protein entatic contribution toward the stabilization and control of an active site metal-ligand bond.

The Fe K-edge absorption spectra for ground-state (GS) and photoexcited-state (600 fs delay) ferrous horse heart cyt c are shown in Fig. 1A. A ground-state contribution, as estimated from the XES data, was subtracted from the photoexcited-state spectrum so as to give the true excited-state (ES) spectrum. The edge, white line, and shape resonances of the ES spectrum shift to lower energy relative to the GS spectrum (Fig. 1A). The spectral changes upon converting from GS to ES are consistent with those exhibited between a six-coordinate LS and a five-coordinate HS complex (fig. S1). The spectra were modeled by using MXAN (multiple scattering) calculations (26, 27) of DFT-generated structures based on the active site model in Fig. 1B. The best fits to both the GS and ES data, along with the structural parameters from the DFT models for each, are shown in Fig. 1, C and D, with the Fe(II)–S(Met) bond length for the GS fixed to match the EXAFS-derived bond distance of 2.29 Å (9). The best simulation was determined by its χ^2 value, as described in supplementary text S.2. The ES structure exhibits loss of the Met ligand (at 2.9 Å) and an elongation of the Fe(II)–N(His) and Fe(II)-N(por) bond lengths, which is consistent with the formation of a five-coordinate, HS heme. MXAN simulations of other DFT models are shown in figs. S2 to S8, where either the Fe(II)–N(His) or Fe(II)–S(Met) bond distances were fixed to different lengths. However, these and other simulations resulted in larger χ^2 values and in particular did not properly reproduce the edge region of the absorption spectrum, as demonstrated by the large residuals in the edge region of those simulations. Therefore, the ES spectrum serves as direct verification of loss of the Fe(II)–S(Met) ligand upon photoexcitation (Fig. 1A, structural insert). The 2.9-Å Fe–S(Met) distance is a lower

limit; simulations with increased Fe–S(Met) distances yield nearly identical residuals (fig. S7).

Kβ x-ray emission spectroscopy (XES) probes the spin state (number of unpaired 3d electrons) of the absorbing metal via the 3p-3d exchange interactions after exciting a 1s electron into the continuum and probing the subsequent 3p → 1s emission (28). These spectra for the GS and ES (at 600 fs time delay) ferrous cyt c are shown in Fig. 2A. Conversion from GS to ES results in a shift in the $K\beta_{1,3}$ peak from ~7058 to ~7060 eV, with a decrease in peak intensity relative to the integrated signal, and the appearance of a Kβ′ feature (because of the strong 3p-3d exchange interaction) at ~7046 eV. Loss of an axial ligand should change the Fe 3d electron configuration from the low-spin $(d_{xy})^2(d_{xz,yz})^4(d_{z^2})^0(d_{x^2-y^2})^0$ to the high-spin$(d_{xy})^2(d_{xz,yz})^2(d_{z^2})^1(d_{x^2-y^2})^1$. Therefore, the spectra reflect a conversion from a singlet (zero unpaired electrons) to a quintet (four unpaired electrons) spin state. Comparable Kβ-XES changes are observed for singlet and quintet Fe(II) model complexes (Fig. 2B), indicating that cyt c changes from singlet to quintet spin state upon photoexcitation of cyt c and correlating with the loss of the axial S(Met) ligand.

The emission spectrum was measured at multiple time delays, from nominal time 0 to 100 ps. Difference spectra (excited – ground state) (Fig. 2, bottom) are shown in Fig. 3A. The individual difference spectra are easily reproduced by including both singlet and quintet spectral contributions (fig. S9). Modeling of the time dependence of the difference spectra (Fig. 3B) indicates that the $S = 2$ state persists out into the picosecond time regime. The low-spin ground state recovery is exponential with a time constant of 6.1 ps, which is consistent with the ligand recovery time reported from OTA and TR^3 measurements (17–19).

Photoexcitation in ferrous cyt c places the system in a hot five-coordinate ground state because of localized heating of the heme (19). The excess kinetic energy from photon absorption that is initially deposited into the heme vibrational energy levels transfers out of the heme into the bulk of the protein with a time constant of 6.4 ps (22). The Fe K-edge XAS and Kβ XES data confirm that the Fe(II)–S(Met) bond is broken upon photo-excitation, and the cyt c heme site adopts a square pyramidal geometry with an $S = 2$ spin state. The singlet and quintet potential energy surfaces cross when the Fe–S(Met) distance is ~3 Å. This bond length corresponds to the equilibrium Fe–S(Met) bond length of the five-coordinate HS state, making relaxation to the six-coordinate, LS state barrier-less and allowing for adiabatic transfer between these two surfaces (fig. S10). The Kβ XES kinetics track reformation of the Fe(II)–S(Met) bond by directly quantifying the singlet and quintet species as a function of time (Fig. 3C, inset). Whereas binding a different ligand, such as a lysine (as observed in the alkaline state) or histidine, would also result in a singlet ground state, binding these ligands would require larger protein reorganization to enable close proximity to the heme iron. Carbonmonoxy myoglobin, after photoexcitation and ligand loss, exhibits biexponential protein tertiary reorganization with 74-ps and 2.7-ns time constants, which are significantly longer than the 6.1-ps time constant for recovery of the cyt c singlet state (29). Assuming comparable protein reorganization times for cyt c, on the ultrafast time scale of bond loss and geminate recombination, an additional ligand cannot bind to Fe, so the active site remains five-coordinate until the Met rebinds. Presuming

thermal equilibrium between the five-coordinate and six-coordinate species after IVR, we can use singlet/quintet populations to determine the strength of the Fe(II)–S(Met) bond in cyt c. The heme temperature as a function of time was obtained by using TR^3 frequency shifts for ferrous cyt c (19), which were converted to temperature by using the frequency-temperature relationship determined by Asher and Murtaugh (30). The equilibrium constant (K_{eq}) values are determined from the relative ratios of quintet to singlet state populations. The resulting Van't Hoff plot (Fig. 3C) provides ΔH and ΔS values of 6.5 ± 1.2 kcal/mol and 16.0 ± 3.2 cal/(mol*K) ($T\Delta S$ ~ 5.2 kcal/mol at RT), respectively. The Fe(II)–S(Met) ΔH for solution-phase Met (a Met that is not constrained to coordinate to the Fe by the protein), determined from DFT calculations correlated to RIXS data, is 2.6 kcal/mol (14); therefore, the protein entatic contribution to the strength of the Fe(II)–S(Met) bond is ~4 kcal/mol of the total ΔH.

Because the weak Fe–S(Met) bond in ferrous cyt c is stabilized by the protein, the Met remains bound under physiological conditions when cyt c functions as an ET protein but is lost under CL bound apoptotic conditions. The dominant contribution to this stabilization likely comes from the –OH group of Tyr67, which forms a hydrogen bonding network that encompasses Met80, a bound H_2O molecule, Asn52, and Thr78 (Fig. 3D). This network is conserved across various forms of cyt c (31), providing steric and electronic contributions to maintaining the Fe(II)–S(Met) bond. Our estimate of ~4 kcal/mol for the entatic contribution is consistent with DFT calculations of 3 kcal/mol for the Tyr-OH–S(Met) bond strength (fig. S11), as well as experimental measurements of the hydrogen bond strength between methanol and dimethylthioether (32). This limited entatic contribution to the total bond strength suggests that the Fe–S(Met) bond can be broken by interrupting the hydrogen bonding network connected to the S(Met) ligand.

The CL interaction with cyt c initiates apoptosis by stimulating loss of the Fe–S(Met) bond, resulting in a five-coordinate active site that is primed for the peroxidation of the CL. This can also occur in ferrocytochrome c because CL can cause Met loss and tune the Fe redox potential for oxidation under aerobic conditions (33). On a molecular level, the extended-lipid anchorage model (34) is typically proposed, in which CL binds to cyt c through electrostatic and hydrogen bonding interactions. Recent crystal structures of yeast iso-1–cyt c show that docked linoleic acid interacts with Asn52 and sits adjacent to the Tyr67 and heme (35). Thus, the linoleic acid can interrupt the internal hydrogen bonding network by interactions with either of these residues. Loss of the Fe–S (Met) bond results in protein conformational changes, with the active site ultimately in equilibrium with a five-coordinate, high-spin iron center (36, 37). Thus, the hydrogen bonding network connected to the Met80 ligand helps stabilize the native conformation, but the protein stabilization of ~4 kcal/mol gives a total bond strength that is easily overcome by the enthalpy of binding of CL [~15 kcal/mol for dioleoylphosphatidylglycerol (38)], causing Fe–S(Met) bond dissociation and protein conformational reorganization.

Given the large size as well as the large number of secondary and tertiary interactions of a protein relative to a typical metal complex, it is somewhat surprising to obtain a protein entatic stabilization as limited as 4 kcal/mol. In this respect, it is valuable to compare this energy with computational values predicted for other systems. A comparable effect has been

observed in binuclear type 3 Cu proteins; hemocyanin (Hc) has a higher binding affinity for dioxygen than the multicopper oxidases (MCOs). Hc was shown to have a much shorter Cu-Cu distance than the MCO (4.2 versus 6.5 Å), and DFT calculations indicate that this increases the electrostatic repulsion in the former, destabilizing its deoxy form by ~6 kcal/mol and leading to favorable O_2 binding (39). Iron-containing zeolites exhibit excellent reactivity in the hydroxylation of methane to methanol at the α-O site. This ^{5}Fe(IV)=O species, which is active toward hydrogen atom abstraction (HAA) from methane, is destabilized by ~5 kcal/mol because of lattice constraints, effectively lowering the activation barrier for HAA and greatly increasing reactivity (40). The experimental value presented here is consistent with these computational estimates. While 4 to 6 kcal/mol is rather small in protein terms, these energies are quite accessible and appear to be critical for performing and optimizing chemical function.

Supplementary Material

Refer to Web version on PubMed Central for supplementary material.

Acknowledgments

Use of the Linac Coherent Light Source (LCLS) and the Stanford Synchrotron Radiation Lightsource (SSRL) of the SLAC National Accelerator Laboratory is supported by the U.S. Department of Energy (DOE), Office of Science, Office of Basic Energy Sciences under contract DE-AC02-76SF00515. The SSRL Structural Molecular Biology Program is supported by the DOE Office of Biological and Environmental Research and by the National Institutes of Health, National Institute of General Medical Sciences (P41GM103393). This research was supported by the National Institute of General Medical Sciences of the National Institutes of Health under award R01GM040392 (E.I.S.). R.W.H., K.K., and K.J.G. acknowledge support from the Atomic, Molecular, and Optical Sciences program within the Chemical Sciences, Geosciences, and Biosciences Division of the Office of Basic Energy Sciences, Office of Science, DOE. M.E.R. acknowledges the Swiss National Science Foundation, project 158890. H.L. acknowledges an Abbott Laboratories graduate fellowship. R.G.H. is currently an Enrico Fermi Fellow at Argonne National Laboratory. All data are reported in the main text, figures, and supplementary material.

REFERENCES AND NOTES

1. Scott, RA., Mauk, AG. Cytochrome C: A Multidisciplinary Approach. University Science Books; 1996.
2. Pettigrew, GW., Moore, GR. Cytochromes c: Biological Aspects. Springer-Verlag; 1987.
3. Liu J, et al. Chem Rev. 2014; 114:4366–4469. [PubMed: 24758379]
4. Ghosh S, et al. Proc Natl Acad Sci USA. 2009; 106:4969–4974. [PubMed: 19282479]
5. Gray HB, Malmström BG, Williams RJP. J Biol Inorg Chem. 2000; 5:551–559. [PubMed: 11085645]
6. Tsai ML, et al. Proc Natl Acad Sci USA. 2013; 110:14658–14663. [PubMed: 23964128]
7. Kagan VE, et al. Nat Chem Biol. 2005; 1:223–232. [PubMed: 16408039]
8. Ow YP, Green DR, Hao Z, Mak TW. Nat Rev Mol Cell Biol. 2008; 9:532–542. [PubMed: 18568041]
9. Cheng MC, Rich AM, Armstrong RS, Ellis PJ, Lay PA. Inorg Chem. 1999; 38:5703–5708.
10. Tezcan FA, Winkler JR, Gray HB. J Am Chem Soc. 1998; 120:13383–13388.
11. Moore GR, Williams RJP. Eur J Biochem. 1980; 103:513–521. [PubMed: 6244160]
12. Moore GR, Williams RJP. Eur J Biochem. 1980; 103:523–532. [PubMed: 6244161]
13. Raphael AL, Gray HB. Proteins. 1989; 6:338–340. [PubMed: 2560194]
14. Kroll T, et al. J Am Chem Soc. 2014; 136:18087–18099. [PubMed: 25475739]
15. Solomon EI, Hadt RG. Coord Chem Rev. 2011; 255:774–789.

16. Solomon EI, Szilagyi RK, DeBeer George S, Basumallick L. Chem Rev. 2004; 104:419–458. [PubMed: 14871131]
17. Bräm O, Consani C, Cannizzo A, Chergui M. J Phys Chem B. 2011; 115:13723–13730. [PubMed: 22004429]
18. Wang W, et al. J Phys Chem B. 2000; 104:10789–10801.
19. Negrerie M, Cianetti S, Vos MH, Martin JL, Kruglik SG. J Phys Chem B. 2006; 110:12766–12781. [PubMed: 16800612]
20. Henry ER, Eaton WA, Hochstrasser RM. Proc Natl Acad Sci USA. 1986; 83:8982–8986. [PubMed: 3024159]
21. Li P, Champion PM. Biophys J. 1994; 66:430–436. [PubMed: 8161696]
22. Zhang Y, Straub JE. J Phys Chem B. 2009; 113:825–830. [PubMed: 19115811]
23. Kitagawa, T., Spiro, TG., editors. Biological Applications of Raman Spectroscopy. Vol. 3. Wiley; 1988. p. 97-131.
24. Bressler, Ch, et al. Science. 2009; 323:489–492. [PubMed: 19074309]
25. Zhang W, et al. Nature. 2014; 509:345–348. [PubMed: 24805234]
26. Benfatto M, Della Longa S. J Synchrotron Radiat. 2001; 8:1087–1094. [PubMed: 11486360]
27. Benfatto M, Longa SD, D'Angelo P. Phys Scr. 2005; 2005:28.
28. Glatzel P, Bergmann U. Coord Chem Rev. 2005; 249:65–95.
29. Cho HS, et al. Proc Natl Acad Sci USA. 2010; 107:7281–7286. [PubMed: 20406909]
30. Asher SA, Murtaugh J. J Am Chem Soc. 1983; 105:7244–7251.
31. Zaidi S, Hassan MI, Islam A, Ahmad F. Cell Mol Life Sci. 2014; 71:229–255. [PubMed: 23615770]
32. Howard DL, Kjaergaard HG. Phys Chem Chem Phys. 2008; 10:4113–4118. [PubMed: 18612514]
33. Serpas L, Milorey B, Pandiscia LA, Addison AW, Schweitzer-Stenner R. J Phys Chem B. 2016; 120:12219–12231. [PubMed: 27934230]
34. Tuominen EKJ, Wallace CJA, Kinnunen PKJ. J Biol Chem. 2002; 277:8822–8826. [PubMed: 11781329]
35. McClelland LJ, et al. J Am Chem Soc. 2016; 138:16770–16778. [PubMed: 27990813]
36. Capdevila DA, et al. Biochemistry. 2015; 54:7491–7504. [PubMed: 26620444]
37. Pandiscia LA, Schweitzer-Stenner R. J Phys Chem B. 2015; 119:12846–12859. [PubMed: 26369421]
38. Zhang F, Rowe ES. Biochim Biophys Acta. 1994; 1193:219–225. [PubMed: 8054342]
39. Yoon J, Fujii S, Solomon EI. Proc Natl Acad Sci USA. 2009; 106:6585–6590. [PubMed: 19346471]
40. Snyder BER, et al. Nature. 2016; 536:317–321. [PubMed: 27535535]

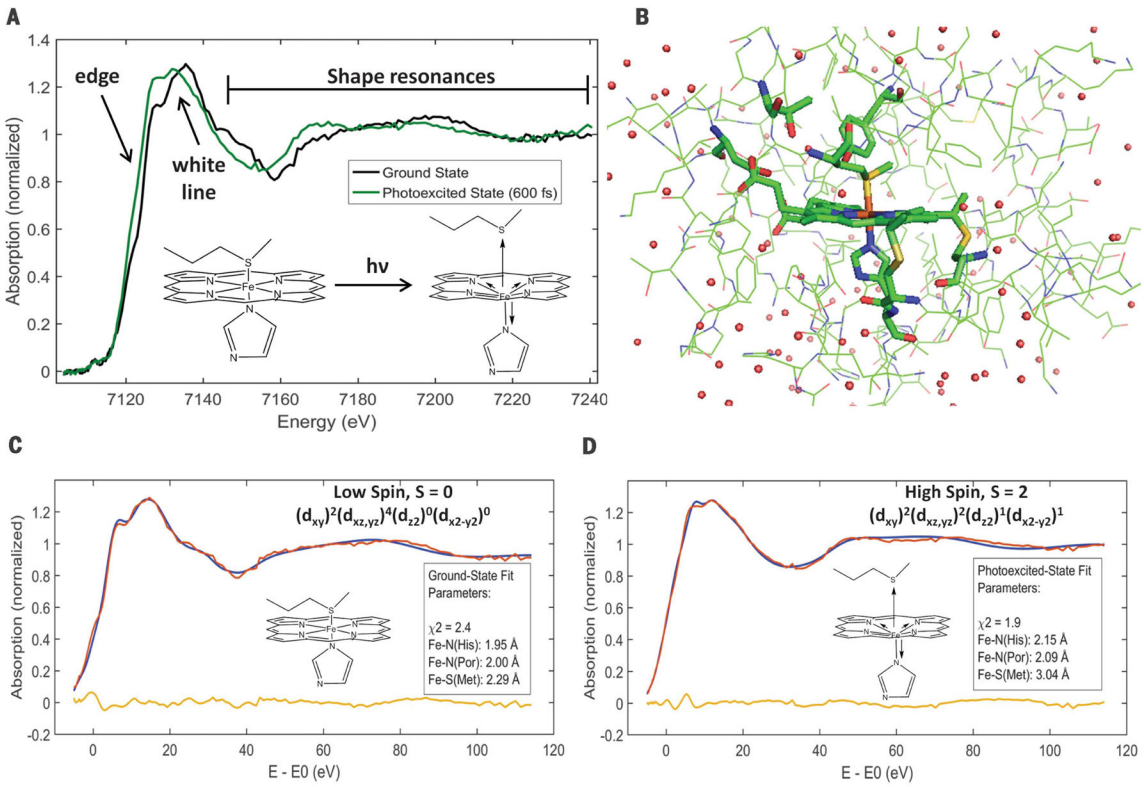

Fig. 1. Ultrafast x-ray absorption spectra of ferrous cytochrome c

(**A**) Superimposed spectra of ground-state (black) and excited-state (green) cyt c, showing the edge, white line, and shape resonance regions. (**B**) cyt c heme structural model used in MXAN simulations. (**C**) Fit (blue) to the GS spectrum (red) and associated structural parameters, derived from MXAN simulation. (**D**) Fit (blue) to the ES spectrum (red) and associated structural parameters, derived from MXAN simulation. The fit residuals are given at the bottom of (C) and (D), and the structural models that fit the spectra are shown above the residuals.

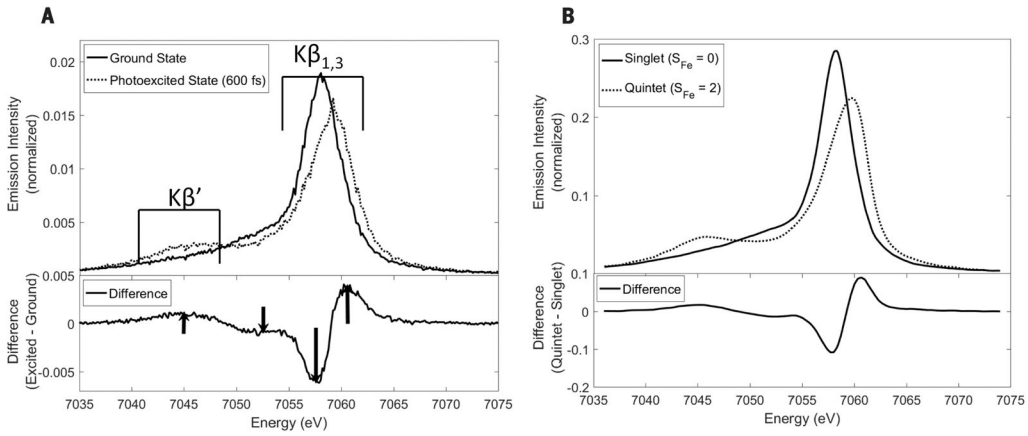

Fig. 2. Ultrafast Kβ XES of ferrous cytochrome c

(**A**) Kβ x-ray emission spectra of ground (solid) and excited-state (dashed) cyt c after excitation at 520 nm (spectra are normalized to the integrated intensity). (Bottom) The difference of the photoexcited and ground-state XES. The arrows indicate positive and negative differences. (**B**) Singlet {[Fe(II)(2,2′-bipyridine)$_3$]$^{2+}$, solid} and quintet {[Fe(II)(phenanthroline)$_2$(NCS)$_2$], dashed} reference spectra used to model cyt c Kβ XES (25). The Kβ XES measures spin state (28) and is not sensitive to specific ligation for Fe(II) complexes with $S = 0$ and $S = 2$.

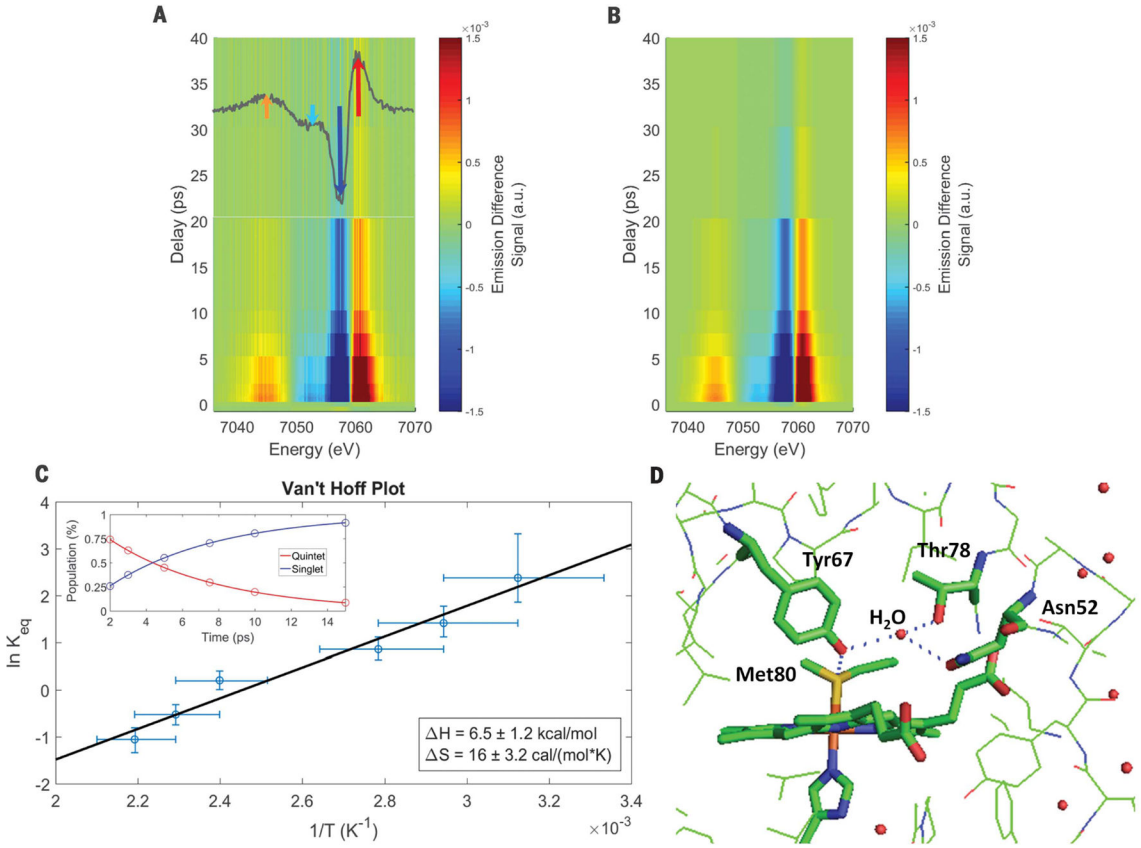

Fig. 3. Excited state time evolution and thermal decay analysis.<

br>(**A**) Time evolution of the Kβ x-ray emission difference (excited – ground state) spectra; the spectra are plotted with energy on the x axis and delay time on the y axis, and the difference intensity is given by the color scheme to the right, with red and blue signifying positive and negative difference signals, respectively. (**B**) Modeling of the Kβ XES difference spectrum by using only singlet and quintet spectra and a lifetime of 6.1 ps, as described in supplementary materials (supplementary text S.1.6 and fig. S9). (**C**) Van't Hoff plot used to determine bond thermodynamics. (Inset) Populations of singlet (blue) and quintet (red) species obtained from XES modeling. Error bars reflect ± 1 cm^{-1} error in resonance Raman frequencies and ± 5% error in quintet populations. (**D**) Cyt c hydrogen bonding interactions (blue dashed lines) that stabilize Fe-S(Met) bonding. Hydrogens are omitted for clarity.